6056 *Inorg. Chem.* **2000,** *39,* 6056−6060

A New Inorganic−Organic Hybrid Iron(III) Arsenate: $(C_2H_{10}N_2)[Fe(HAsO_4)_2(H_2AsO_4)](H_2O)$. Hydrothermal Synthesis, Crystal Structure, and Spectroscopic and Magnetic Properties

Begoña Bazán,[‡] José L. Mesa,[†] José L. Pizarro,[‡] L. Lezama,[†] María I. Arriortua,[‡] and Teófilo Rojo*,[†]

Departamento de Química Inorgánica and Departamento de Mineralogía-Petrología,
Facultad de Ciencias, Universidad del País Vasco, Apdo. 644, E-48080 Bilbao, Spain

Received July 25, 2000

A new iron(III) arsenate templated by ethylenediamine, $(C_2H_{10}N_2)$ $[Fe(HAsO_4)_2(H_2AsO_4)](H_2O)$, has been prepared by hydrothermal synthesis. The unit-cell parameters are $a = 8.705(3)$ Å, $b = 16.106(4)$ Å, $c = 4.763(1)$ Å, $\beta = 90.63(3)°$; monoclinic, $P2_1$ with $Z = 2$. The compound exhibits a chain structure along the *c*-axis with the ethylenediammonium cations as counterion. The chains show isolated FeO_6 octahedra with two $HAsO_4$ and one H_2AsO_4 tetrahedra per FeO_6 octahedron. The ESR spectrum at 5.0 K is isotropic with a *g*-value of 2.0, which remains practically unchanged at room temperature. Magnetic measurements indicate the presence of antiferromagnetic interactions. A value of −0.835 K for the *J*-exchange parameter has been calculated by fitting the magnetic data to a model for antiferromagnetic chains of spin $S = 5/2$.

Introduction

The world of crystalline porous materials has long been dominated by aluminosilicate zeolites, which are used widely in catalysis, separations, and ion-exchange processes.[1] The discovery of new families of porous materials, including new crystalline systems as well as amorphous mesoporous materials, has raised hopes that such materials could be tailored for new applications, for example, in sensors and nanotechnology. Consequently, there has been tremendous interest in novel porous solids, both inorganic and organic.[2] A frequently used concept in seeking systematic trends in this area of materials chemistry is that of templating, the tendency of a cation to direct the reaction to form a particular product.[3] In this way, small organic molecules, particularly those containing protonated amino groups, have played an outstanding role in templating novel networks[4] such as oxides, phosphates, and phosphonates with a large variety of transitions metal ions.[5−11]

Although designing phases similar to aluminosilicate zeolitic structures has been the subject of main interest in the study of these materials, the discovery of new compounds with novel structural features has also assumed an important role.[2,12,13] Among the open-framework materials, metal phosphates occupy a major position. A number of works dealing with organically templated iron phosphates has evidenced a rich structural chemistry in this system.[14−20] Open-framework cobalt(II) phosphates have been also synthesized and studied.[9,21] Recently, two antiferromagnets, layered Mn(II)−phosphate and −phosphite templated by ethylenediamine, have been prepared and their properties reported.[22,23] Furthermore, several arsenate compounds with paramagnetic metal ions and templated by diammonium cations have also been reported.[24−26] However these

---

* To whom all correspondence should be addressed. Tel: 34-946012458. Fax: 34-944648500. E-mail: qiproapt@lg.ehu.es.

[†] Departamento de Química Inorgánica.

[‡] Departamento de Mineralogía-Petrología.

(1) Davis, M. E. *Chem. Eur. J.* **1997**, *3*, 1745.
(2) Cheetham, A. K.; Férey, G.; Loiseau, T. *Angew. Chem., Int. Ed. Engl.* **1999**, *38*, 3268.
(3) Davis, M. E.; Lobo, R. F. *Chem. Mater.* **1992**, *4*, 756.
(4) Lawton, S. L.; Rohrbaugh, W. J. *Science* **1990**, *247*, 1319.
(5) Haushalter, R.; Mundi, L. *Chem. Mater.* **1992**, *4*, 31.
(6) Soghomonian, V.; Chen, Q.; Haushalter, R.; Zubieta, J. *Chem. Mater.* **1993**, *5*, 1690.
(7) Kahn, M.; Lee, Y.; O'Connor, C.; Haushalter, R.; Zubieta, J. *J. Am. Chem. Soc.* **1994**, *116*, 4525.
(8) Zapf, P.; Rose, D.; Haushalter, R.; Zubieta, J. *J. Solid State Chem.* **1996**, *125*, 182.
(9) BeBord, J.; Haushalter, R.; Zubieta, J. *J. Solid State Chem.* **1996**, *125*, 270.
(10) Dhingra, S.; Haushalter, R. *J. Chem. Soc., Chem. Commun.* **1993**, *21*, 1665.
(11) Zhang, Y.; O'Connor, C.; Clearfield, A.; Haushaletr, R. *Chem. Mater.* **1996**, *8*, 595.
(12) Choudhury, A.; Natarajan, S.; Rao, C. N. R. *J. Solid State Chem.* **1999**, *146*, 538.
(13) Cavellec, M. R.; Riou, D.; Ferey, G. *Inorg. Chim. Acta* **1999**, *291*, 317.
(14) Lii, K.-H.; Huang, Y.-F.; Zima, V.; Huang, C.-Y.; Lin, H.-M.; Jiang, Y.-C.; Liao, F.-L.; Wang, S.-L. *Chem. Mater.* **1998**, *10*, 2599.
(15) Cavellec, M.; Riou, D.; Greneche, J. M.; Ferey, G. *Inorg. Chem.* **1997**, *36*, 2181.
(16) DeBord, J. R. D.; Reiff, W. M.; Warren, C. J.; Haushalter, R.; Zubieta, J. *Chem. Mater.* **1997**, *9*, 1994.
(17) Lii, K. H.; Huang, Y. F. *J. Chem. Soc., Chem. Commun.* **1997**, 1311.
(18) Zima, V.; Lii, K.-H.; Nguyen, N.; Ducouret, A. *Chem. Mater.* **1998**, *10*, 1914.
(19) DeBord, J.; Reiff, W.; Haushalter, R.; Zubieta, J. *J. Solid State Chem.* **1996**, *125*, 186.
(20) Lii, K.-H.; Huang, Y.-F. *J. Chem. Soc., Dalton Trans.* **1997**, 2221.
(21) Chen, J.; Jones, R. H.; Natarajan, S.; Hursthouse, M. B.; Thomas J. M. *Angew. Chem., Int. Ed. Engl.* **1994**, *33*, 639.
(22) Escobal, J.; Pizarro, J. L.; Mesa, J. L.; Lezama, L.; Olazcuaga, R.; Arriortua, M. I.; Rojo, T. *Chem. Mater.* **2000**, *12*, 376.
(23) Fernandez, S.; Mesa, J. L.; Pizarro, J. L.; Lezama, L.; Arriortua, M. I.; Olazcuaga, R.; Rojo, T. *Chem. Mater.* **2000**, *12*, 2092.
(24) Haushalter, R. C.; Wang, Z.; Meyer, L. M.; Dhinga, S. S.; Thompson, M. E.; Zubieta, J. *Chem. Mater.* **1994**, *6*, 1463.
(25) Liu, A.-H.; Wang, S.-L. *Inorg. Chem.* **1998**, *37*, 3415.
(26) Tsai, Y.-M.; Wang, S.-L.; Huang, C.-H.; Lii, K.-H. *Inorg. Chem.* **1999**, *38*, 4183

10.1021/ic000835a CCC: $19.00

materials have not been studied in depth, as have the related phosphate compounds.

In this work we report on the hydrothermal synthesis, crystal structure, and spectroscopic and magnetic properties of a new iron(III) arsenate templated by ethylenediammonium cations, $(C_2H_{10}N_2)$ $[Fe(HAsO_4)_2(H_2AsO_4)](H_2O)$. This compound is the first reported iron(III)−arsenate templated by ethylenediamine.

Experimental Section

Synthesis and Characterization. $(C_2H_{10}N_2)[Fe(HAsO_4)_2(H_2AsO_4)](H_2O)$ was prepared from reaction mixtures of As_2O_5 (0.375 mmol), ethylenediamine (0.269 mmol), and $FeCl_3\cdot 6H_2O$ (0.009 mmol), in a mixture of ca. 30 mL of water and 1-butanol (volume ratio 1:4). The initial pH of the reaction mixture was ca. 3. The synthesis was carried out in a poly(tetrafluoroethylene)-lined stainless steel container under autogenous pressure, filled to ca. 75% volume capacity, and all reactants were stirred briefly before heating. The reaction mixture was heated at 170 °C for 5 days, followed by slow cooling to room temperature. The pH of the reaction increased up to ca. 5. The resulting product was filtered off, washed with ether, and dried in air. Well-formed prismatic single crystals with light green color appeared in the preparation. The metal ion and arsenic contents were confirmed by inductively coupled plasma atomic emission spectroscopy (ICP-AES) analysis performed with a ARL Fisons 3410 spectrometer. C, H, and N elemental analysis was carried out with a Perkin-Elmer Model 240 automatic analyzer. Found: Fe, 9.9; As, 40.1; C, 4.1; H, 2.6; N, 4.7. $(C_2H_{10}N_2)[Fe(HAsO_4)_2(H_2AsO_4)](H_2O)$ requires: Fe, 10.0; As, 40.4; C, 4.3; H, 2.9; N, 5.0. The density, 2.7(1) g cm^{-3}, was measured by flotation in a mixture of CH_2I_2/CCl_4.

Thermal Decomposition. Thermogravimetric measurements were carried out heating the sample at 5 °C min^{-1} under air atmosphere in the 30−800 °C range by using a SDC 2960 Simultaneous DSC-TGA TA instrument. The decomposition curve reveals a continuous weight loss (ca. 14.3%) between 150 and 270 °C. This fact can be attributed to the simultaneous loss of the ethylenediammonium cation and the water molecule present in the compound (calc 14.4%). After this process, the decomposition of the hydrogen- and dihydrogenarsenate anions occurs between 270 and 560 °C. Above 560 °C, additional weight loss is not observed in the thermogravimetric curve. The X-ray pattern diffraction of the residue obtained from the thermogravimetric analysis shows the presence of peaks which can be indexed with the unit cell parameters of $Fe(AsO_4)$,[27] $a = 7.56(1)$ Å, $b = 8.08(1)$ Å, $c = 5.01$ Å, and $\beta = 104.5(1)°$. Furthermore, different peaks with low intensity (ca. 5%) appear at $2\theta = 25.55°$, 30.13°, and 32.06°. These peaks were assigned to the Fe_2O_3 phase in its maghemite-C synthetic form.[27]

The thermal behavior of $(C_2H_{10}N_2)[Fe(HAsO_4)_2(H_2AsO_4)](H_2O)$ has also been followed by using time-resolved X-ray thermodiffractometry. The patterns were performed in air atmosphere with a PHILIPS X'PERT automatic diffractometer (Cu Kα radiation) equipped with a variable-temperature stage (Anton Paar HTK16) and a Pt sample holder. The data were recorded in 2θ steps of 0.02° in the range $5° \leq 2\theta \leq 50°$, counting for 1 s per step and increasing the temperature at 5 °C min^{-1} from room temperature up to 650 °C. The results are given in Figure 1. The compound is stable up to ca. 75 °C. The intensity of the monitored (100), (020), and (110) peaks remains practically unchanged. However, a splitting of these peaks occurs in the 100−200 °C range, suggesting the existence of a structural change before the thermal decomposition of the compound. At approximately 225 °C the peaks of the X-ray powder diffractogram practically disappear, indicating the decomposition of the compound. Between ca. 500 and 650 °C, peaks belonging to the $Fe(AsO_4)$ arsenate were observed. Furthermore, a minor proportion of the maghemite-C synthetic Fe_2O_3 phase is also detected (see inset in Figure 1), in good agreement with the thermogravimetric data.

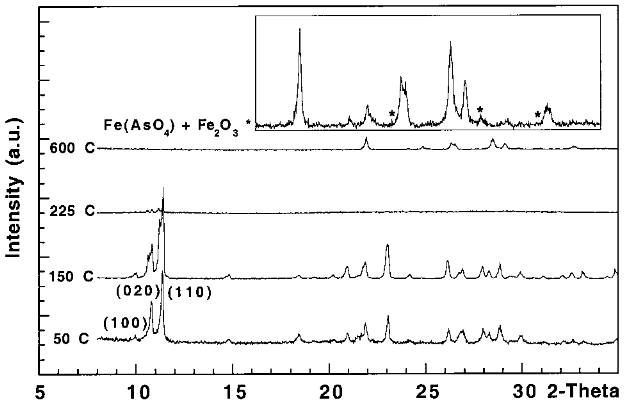

Figure 1. Thermodiffractograms of $(C_2H_{10}N_2)[Fe(HAsO_4)_2(H_2AsO_4)](H_2O)$. The * given in the inset corresponds to the Fe_2O_3 phase.

Table 1. Crystallographic Data for $(C_2H_{10}N_2)[Fe(HAsO_4)_2(H_2AsO_4)](H_2O)$

formula	$C_2H_{16}N_2O_{13}As_3Fe$
a, Å	8.705(3)
b, Å	16.106(4)
c, Å	4.763(1)
β, deg	90.63(3)
V, Å^3	666.7(3)
Z	2
fw (g mol^{-1})	556.8
space group	$P2_1$ (no. 4)
T, °C	20
radiation, λ(Mo Kα), Å	0.71073
ρ_{obsd}, ρ_{calcd}, g cm^{-3}	2.7(1), 2.770
μ(Mo Kα), mm^{-1}	8.581
R $[I > 2\sigma(I)]^a$	R1 = 0.027, wR2 = 0.050
R [all data]	R1 = 0.037, wR2 = 0.051

[a] $R1 = [\sum(|F_o| - |F_c|)]/\sum|F_o|$; $wR2 = [\sum[w(|F_o|^2 - |F_c|^2)^2]/\sum[w(|F_o|^2)^2]]^{1/2}$; $w = 1/[\sigma^2|F_o|^2 + (xp)^2]$; where $p = [|F_o|^2 + 2|F_c|^2]/3$; $x = 0.0223$.

Single-Crystal X-ray Diffraction. A suitable single crystal of $(C_2H_{10}N_2)[Fe(HAsO_4)_2(H_2AsO_4)](H_2O)$ with dimensions 0.4 × 0.1 × 0.05 mm was carefully selected under a polarizing microscope and mounted on a glass fiber. Diffraction data were collected at room temperature on an STOE IPDS (Imaging Plate Diffraction System) automated diffractometer using graphite-monochromated Mo Kα. Crystallographic data are reported in Table 1.

A total of 7088 reflections were measured in the range $3.45° \leq \theta \leq 26.03°$. A total of 2407 reflections were independent ($R_{int} = 0.03$) and 2081 observed applying the criterion $I > 2\sigma(I)$. Correction for Lorentz and polarization effects were done[28] and also for absorption taking into account the crystal shape by using the XRED program.[29] The structure was solved by the Patterson method (SHELXS 86 program[30]) and then refined by the full-matrix least-squares method based on F^2, using the SHELXL 97 computer program.[31] The scattering factors were taken from ref 32. All non-hydrogen atoms were assigned anisotropic thermal parameters. Hydrogen atoms were geometrically placed, except for the water molecules, which were not located. The final R factors were R1 = 0.027 [wR2 = 0.050]. Maximum and minimum peaks in final difference synthesis were 0.560, −0.881 e Å^{-3}. The final atomic coordinates and thermal parameters have been deposited at the Cambridge Crystallographic Data Centre (CCDC 150503). All drawings were made using ATOMS and ORTEP programs.[33,34] Selected bond distances and angles are given in Table 2.

---

(27) Powder Diffraction File−Inorganic and Organic, Files No., 21-910 and 39-1346, Pennsylvania, PA, 1995.

(28) *Stoe IPDS Software*, Version 2.87; Stoe & Cie: Darmstadt, Germany, 1998.

(29) *XRED*; Stoe & Cie GmbH: Darmstadt, Germay, 1998

(30) Sheldrick, G. M. *Acta Crystallogr.* **1990**, *A46*, 467.

(31) Sheldrick, G. M. SHELXL 97: *Program for the Refinement of Crystal Structures;* University of Göttingen: Germany, 1997.

(32) *International Tables for X-ray Crystallography*; Kynoch Press: Birmingham, England, 1974; Vol. IV, p 99.

(33) Dowty, E. *ATOMS*: *A Computer Program for Displaying Atomic Structures*; Shape Software: 521 Hidden Valley Road, Kingsport, TN, 1993.

Table 2. Selected Bond Distances (Å) and Angles (deg) for $(C_2H_{10}N_2)[Fe(HAsO_4)_2(H_2AsO_4)](H_2O)$ (esd's in Parentheses)[a]

Bond Distances (Å)

FeO_6 octahedron

Fe−O(1)	2.027(4)
Fe−O(3)^{i}	2.026(4)
Fe−O(6)	1.998(4)
Fe−O(7)^{ii}	1.993(4)
Fe−O(9)	2.007(5)
Fe−O(11)^{i}	2.013(5)

As(1)O$_4$ tetrahedron		As(2)O$_4$ tetrahedron		As(3)O$_4$ tetrahedron	
As(1)−O(1)	1.668(4)	As(2)−O(5)	1.731(4)	As(3)−O(9)	1.660(4)
As(1)−O(2)	1.680(4)	As(2)−O(6)	1.667(4)	As(3)−O(10)	1.725(4)
As(1)−O(3)	1.667(4)	As(2)−O(7)	1.675(4)	As(3)−O(11)	1.663(4)
As(1)−O(4)	1.736(4)	As(2)−O(8)	1.680(4)	As(3)−O(12)	1.707(5)

$(H_3N(CH_2)_2NH_3)^{2+}$

N(1)−C(1)	1.475(9)	N(2)−C(2)	1.491(9)	C(1)−C(2)	1.52(1)

Bond Angles (deg)

FeO_6 octahedron

O(6)−Fe−O(1)	91.9(2)
O(6)−Fe−O(3)^{i}	88.6(1)
O(6)−Fe−O(7)^{ii}	90.7(2)
O(6)−Fe−O(11)^{i}	91.6(2)
O(9)−Fe−O(1)	87.8(2)
O(9)−Fe−O(3)^{i}	89.3(2)
O(9)−Fe−O(7)^{ii}	91.4(2)
O(9)−Fe−O(11)^{i}	88.5(2)
O(1)−Fe−O(3)^{i}	89.4(2)
O(1)−Fe−O(7)^{ii}	89.2(2)
O(3)^{i}−Fe−O(11)^{i}	86.5(2)
O(7)^{ii}−Fe−O(11)^{i}	94.8(2)
O(1)−Fe−O(11)^{i}	174.6(2)
O(3)^{i}−Fe−O(7)^{ii}	178.5(2)
O(6)−Fe−O(9)	177.9(2)

As(1)O$_4$ tetrahedron		As(2)O$_4$ tetrahedron	
O(1)−As(1)−O(2)	107.8(2)	O(5)−As(2)−O(6)	101.0(2)
O(1)−As(1)−O(3)	121.0(2)	O(5)−As(2)−O(7)	110.2(2)
O(1)−As(1)−O(4)	108.2(2)	O(5)−As(2)−O(8)	107.1(2)
O(2)−As(1)−O(3)	110.5(2)	O(6)−As(2)−O(7)	117.2(2)
O(2)−As(1)−O(4)	107.1(2)	O(6)−As(2)−O(8)	112.1(2)
O(3)−As(1)−O(4)	101.2(2)	O(7)−As(2)−O(8)	108.5(2)

As(3)O$_4$ tetrahedron

O(9)−As(1)−O(10)	107.7(2)
O(9)−As(1)−O(11)	120.8(2)
O(9)−As(1)−O(12)	106.6(2)
O(10)−As(1)−O(11)	108.0(2)
O(10)−As(1)−O(12)	105.4(2)
O(11)−As(1)−O(12)	107.3(2)

$(H_3N(CH_2)_2NH_3)^{2+}$

N(1)−C(1)−C(2)	110.2(5)	C(1)−C(2)−N(2)	110.6(6)

[a] Symmetry codes: i = $x, y, z-1$, ii = $x, y, z+1$.

Physical Measurements. The IR spectrum (KBr pellet) was obtained with a Nicolet FT-IR 740 spectrophotometer in the 400−4000 cm^{-1} range. The diffuse reflectance spectrum was registered at room temperature on a Cary 2415 spectrometer in the 5000−50000 cm^{-1} range. A Bruker ESP 300 spectrometer was used to record the ESR polycrystalline spectra at room temperature and 5.0 K. The temperature was stabilized by an Oxford Instrument (ITC 4) regulator. The magnetic field was measured with a Bruker BNM 200 gaussmeter, and the frequency inside the cavity was determined using a Hewlett-Packard 5352B microwave frequency counter. Magnetic measurements of powdered sample were performed in the temperature range 4.2−300 K, using a Quantum Design MPMS-7 SQUID magnetometer. The magnetic field was approximately 0.1 T, a value lying within the range of linear dependence of magnetization vs magnetic field even at 4.2 K.

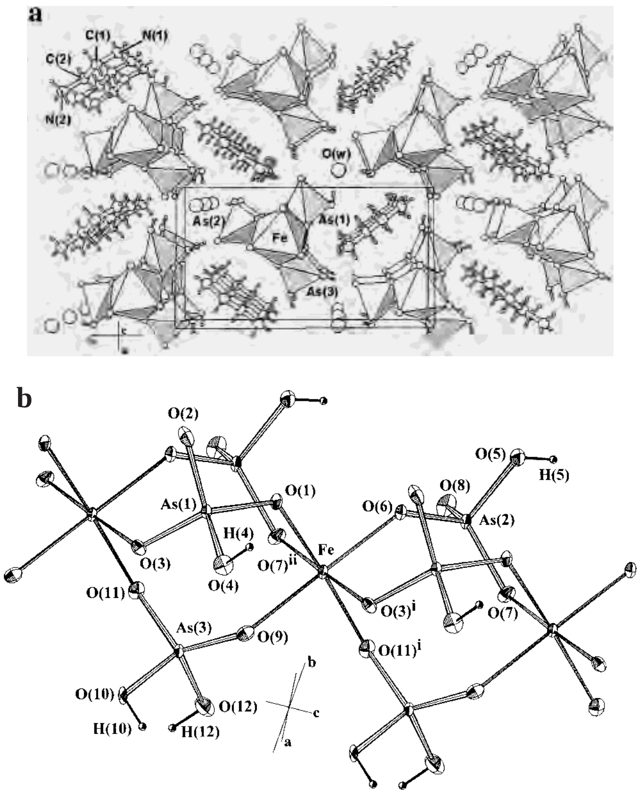

Figure 2. (a) Polyhedral view of $(C_2H_{10}N_2)[Fe(HAsO_4)_2(H_2AsO_4)]$-$(H_2O)$, showing the chain structure. (b) ORTEP drawing (50% thermal ellipsoids) of the $[Fe(HAsO_4)_2(H_2AsO_4)]_n{}^{2n-}$ unit, with detailed labeling of the atoms.

Results and Discussion

Crystal Structure. The structure consists of $[Fe(HAsO_4)_2(H_2AsO_4)]^{2-}$ anionic chains running along the [001] direction. The ethylenediammonium cations are displayed in the cavities of the structure delimited by three different chains and compensating its negative charge (Figure 2a). The water molecules are located in the cavities formed by three arsenate anions belonging to different chains (see Figure 2a). The FeO_6 octahedra are isolated and bridged by two $HAsO_4$ and one H_2AsO_4 tetrahedra. A remarkable structural feature of this compound is the absence of covalent intrachain −Fe−O−Fe− interactions.

Figure 2b shows the isolated $[Fe(HAsO_4)_2(H_2AsO_4)]_n{}^{2n-}$ chains. The FeO_6 octahedra are quite regular with Fe−O distances ranging from 1.993(4) to 2.027(4) Å. As can be seen in Figure 2b the O(1) and O(3)^{i} oxygen atoms in the octahedra are provided by the HOAs(1)O$_3$ tetrahedron with bond distances Fe−O(1) of 2.027(4) and Fe−O(3)^{i} of 2.026(4) Å. The HOAs(2)O$_3$ tetrahedron is bonded to iron(III) cations via O(6) and O(7)^{ii} oxygen atoms with bond distances of 1.998(4) and 1.993(4) Å, respectively. Finally, the O(9) and O(11)^{i} oxygens belonging to the (HO)$_2$As(3)O$_2$ tetrahedron establish bond distances of 2.007(5) and 2.013(5) Å with the iron(III) cation. The *cis*-O−Fe−O angles range from 86.5(2)° to 94.8(2)°, whereas the *trans*-O−Fe−O angles are practically of 180°. The distortion of the FeO_6 polyhedron, from an octahedron ($\Delta = 0$) to a trigonal prism ($\Delta = 1$), calculated by quantification of the Muetterties and Guggenberger description,[35] is $\Delta = 0.01$, which indicates a topology near to octahedron. The Fe(III)−Fe(III) intrachain bond distance is 4.763(1) Å.

---

(34) Johnson, C. K. *ORTEP*, Report ORNL-5138; Oak Ridge National Laboratory: Oak Ridge, TN, 1976.

(35) Muetterties, E. L.; Guggenberger, L. J. *J. Am. Chem. Soc.* **1974**, *96*, 1748.

The $HAsO_4$ and H_2AsO_4 tetrahedra are quite regular, with mean bond distances As−O of 1.69(3) Å. The As(1)−O(4), As(2)−O(5), and As(3)−O(10),O(12) bond distances in the hydrogenarsenate groups are slightly longer (mean value, 1.72(1) Å) than those observed for the other As−O distances (mean value, 1.670(8) Å). The O−As−O angles are in the range from 101.2(2)° to 121.0(2)°. In the ethylenediammonium cations the C−C and C−N bond distances are in the range usually found for this molecule,[36] and the angles are practically similar to that expected for a sp^3 hybridation. The water molecule is linked by two strong hydrogen bonds to the hydrogenarsenate groups. The bond lengths and angles are as follows: $Ow\cdots H(4)^{i}-O(4)-[As(1)]$, 1.897(4) Å, 168.9(4)° ; $Ow\cdots H(5)^{ii}-O(5)-[As(2)]$, 1.955(5) Å, 159.6(3)° [i = x, y, $z+1$; ii = $-x+2$, $y+1/2$, $-z-1$]. Furthermore, the ethylenediammonium cation establishes several hydrogen bonds with the hydrogen- and dihydrogenarsenate groups whose values range from 1.881(5) to 3.184(4) Å. Hydrogen bonds have not been detected between the water molecules and the ethylenediammonium cations.

IR and UV−Vis Spectroscopy. The IR spectrum of $(C_2H_{10}N_2)[Fe(HAsO_4)_2(H_2AsO_4)](H_2O)$ shows the bands corresponding to the vibrations of the water, ethylenediammonium cations, and hydrogen- and dihydrogenarseniate anions. The strong band centered at 3415 cm^{-1} corresponds to the stretching mode of the water molecule. The bending mode of this molecule can be observed at about 1615 cm^{-1}. The stretching mode of the $(NH_3)^+$ group, in the ethylenediammonium cation, appears at 3130 cm^{-1}. The band near 1540 cm^{-1} can be assigned to the $(NH_3)^+$ bending vibration. This band is indicative of the presence of the ethylenediamine molecule in its protonated form,[36,37] in good agreement with the structural results. The stretching vibrations of the $-CH_2-$ groups in the ethylenediammonium appear in the 2930−2600 cm^{-1} range, while the bending modes of these groups can be observed in the 1455−1385 cm^{-1} range. Four different groups of bands can be attributed to the vibrational modes of the $(HAsO_4)^{2-}$ and $(H_2AsO_4)^-$ anions present in the compound.[38] The ν_3 asymmetrical stretching mode [ν_{as}(As−O)] appears at frequencies 870, 825, 760, and 735 cm^{-1}. The ν_1 symmetrical stretch [ν_s(As−O)] is detected at a frequency of 625 cm^{-1}. The asymmetrical deformation vibrations [δ_{as}(O−As−O)] can be observed at 560 and 475 cm^{-1}. Finally, the bands observed at ca. 2360 and 1230 cm^{-1} can be assigned to stretching and bending modes of the HO−As hydrogen- and dihydrogenarsenate anions present in the structure of this compound.

The diffuse reflectance spectrum of this compound exhibits several very weak spin-forbidden d−d bands, at approximately 15 505, 19 800, 22 990, and 26 665 cm^{-1}, as corresponds to a d^5 high-spin cation in an ideal octahedral symmetry.[39]

ESR and Magnetic Properties. The ESR spectrum of $(C_2H_{10}N_2)[Fe(HAsO_4)_2(H_2AsO_4)](H_2O)$ performed at the X-band on a powdered sample at 5.0 K exhibits an isotropic signal in good agreement with the presence of high-spin Fe(III) cations in octahedral symmetry. The g-value is 2.00, and the line width is approximately 430 G. These results are similar to those observed at room temperature, where the g-value and the line width take values of 2.03 and 450 G, respectively.

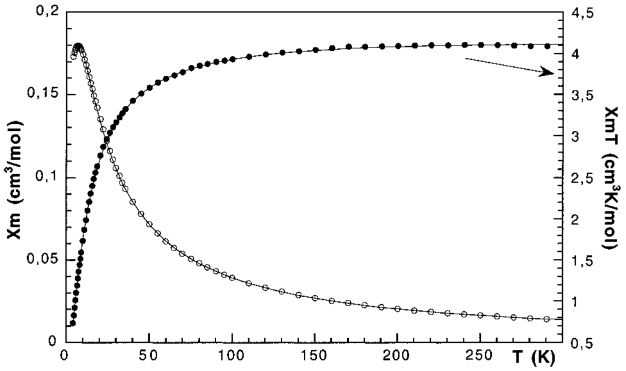

Figure 3. Thermal evolution of the χ_m and χ_mT curves of $(C_2H_{10}N_2)[Fe(HAsO_4)_2(H_2AsO_4)](H_2O)$. The solid lines show the fit of the χ_m and χ_mT experimental data to the model for chains of $S = 5/2$.

Variable-temperature magnetic susceptibility measurements of $(C_2H_{10}N_2)[Fe(HAsO_4)_2(H_2AsO_4)](H_2O)$ have been carried out on a powdered sample from room temperature to 4.2 K. Plots of the χ_m and χ_mT vs T curves are shown in Figure 3. The thermal evolution of χ_m follows the Curie−Weiss law at temperatures higher than 30 K, with $C_m = 4.34$ cm^3 K/mol and $\theta = -13.1$ K. The molar magnetic susceptibility increases from room tempearature with decreasing temperature and reaches a maximum at ca. 8 K, indicating that a long magnetic order is established at this temperature. This result together with the continuous decrease in the χ_mT vs T curve, from 4.089 cm^3 K/mol at room temperature up to 0.736 cm^3 K/mol at 4.2 K, is indicative of antiferromagnetic exchange couplings in the compound.

Considering the structural features of this compound, in which chains of $[Fe(HAsO_4)_2(H_2AsO_4)]^{2-}$ formula run along the [001] direction, the magnetic data have been fitted to the equation given by Fischer and Dingle[40,41] for chains of spin $S = 5/2$, (eq 1):

$$\chi = [Ng^2\beta^2S(S+1)/3kT][(1-n)/(1+n)] \qquad (1)$$

where $n = (T/T_0) - \coth(T_0/T)$ and $T_0 = [2JS(S+1)]/k$, k is Boltzmann's constant, N is Avogadro's number, and β is the Bohr magneton. The best fit (solid lines in Figure 3) is obtained for a value of the J-exchange parameter of $J = -0.835$ K, where $g = 2.0$ obtained from the ESR spectrum. The agreement factor, defined as $F = \sum_i(\chi_{i,obs} - \chi_{i,cal})^2/(\chi_{i,obs})^2$, is 1.03×10^{-4}.

The introduction in eq 1 of a J'-exchange parameter between neighboring chains does not modify in a significant way the obtained results. Consequently, it is possible to conclude that, in this compound, the main magnetic interactions are propagated along the chains through three different superexchange pathways, Fe−O(3)−As(1)−O(1)−Fe, Fe−O(6)−As(2)−O(7)−Fe, and Fe−O(11)−As(3)−O(9)−Fe (see Figure 2b). These pathways present similar Fe−O−As and O−As−O angles with a mean value of 126° and 120°, respectively. In this way, the calculated magnetic exchange parameter, $J = -0.835$ K, represents the mean value corresponding to the exchange pathways that connect the Fe(III) cations in the structure of this compound.

Concluding Remarks

The first iron(III) arsenate templated by ethylenediamine with formula $(C_2H_{10}N_2)[Fe(HAsO_4)_2(H_2AsO_4)](H_2O)$ has been pre-

---

(36) Gharbi, A.; Jouini, A.; Averbuch-Pouchot, M. T.; Durif, A. *J. Solid State Chem.* **1994**, *111*, 330.

(37) Dolphin, D.; Wick, A. E. *Tabulation of Infrared Spectral Data*; John Wiley & Sons: New York, 1977.

(38) Nakamoto, K. *Infrared and Raman Spectra of Inorganic and Coordination Compounds*; John Wiley & Sons: New York, 1997.

(39) Lever, A. B. P. *Inorganic Electronic Spectroscopy*; Elsevier Science Publishers B.V., Amsterdam, Netherlands, 1984.

(40) Fisher, M. E. *Am. J. Phys.* **1964**, *32*, 343.

(41) Dingle, R.; Lines, M. E.; Holt, S. L. *Phys. Rev.* **1969**, *187*, 643.

pared under hydrothermal conditions. The crystal structure consists of inorganic chains of composition $[Fe(HAsO_4)_2(H_2AsO_4)]^{2-}$ in which no covalent intrachain Fe−O−Fe bond is established. Both the ethylenediammonium cations and the water molecules are located between the chains in different cavities of the structure. The thermogravimetric study indicates the loss of ethylenediammonium and water in the 150−270 °C range. The inorganic residue evolution gives as final product a mixture of $Fe(AsO_4)$ and Fe_2O_3. The IR spectrum shows the bands belonging to the ethylenediammonium cation and $(HAsO_4)^{2-}$ and $(H_2AsO_4)^{-}$ anions. The diffuse reflectance and ESR measurements are in good agreement with the existence of a d^5 high-spin Fe(III) cation in octahedral symmetry. The best fit of the magnetic data was carried out by using a model for chains of spin $S = 5/2$. The J/K value was -0.835 K.

Acknowledgment. This work was financially supported by the Ministerio de Educación y Ciencia and Universidad del País Vasco/EHU (Grants PB97-0640 and 169.310-EB149/98, respectively), which we gratefully acknowledge. We thank Dpto. Física de la Materia Condensada of the UPV/EHU for use of the STOE IPDS automatic diffractometer and E. Marquestaut (ICMCB, Pessac, France) for ESR measurements. B.B. thanks the UPV/EHU for a doctoral fellowship.

Supporting Information Available: Four X-ray crystallographic files, in CIF format, are available. This material is available free of charge via the Internet at http://pubs.acs.org.

IC000835A